Optimization and modeling of diananofiltration process for the detoxification of ligno-cellulosic hydrolysates - Study at pre-industrial scale

D.T.N.N. Nguyen, M. Lameloise, Wafa Guiga, R. Lewandowski, M. Bouix, C. Fargues

Optimization and modeling of diananofiltration process for the detoxification of ligno-cellulosic hydrolysates - Study at pre-industrial scale

Nguyen D.T.N.N.[1], Lameloise M.-L.[1], Guiga W. [1, 3], Lewandowski R. [1], Bouix M. [4], Fargues C. [1, 2]

[1] UMR Ingénierie Procédés Aliments, AgroParisTech, Inra, Université Paris-Saclay, 91300 Massy, France

[2] Université Paris Sud, 91400 Orsay, France

[3] Cnam, UMR Ingénierie Procédés Aliments, France 75003 Paris, France

[4] UMR Génie et Microbiologie des Procédés Alimentaires, AgroParisTech, Inra, Université Paris-Saclay, 78850 Thiverval-Grignon, France

Correspondence: Claire FARGUES, AgroParisTech, UMR 1145 Ingénierie Procédés Aliments, 1 av des Olympiades, F-91300 Massy, France.
Phone: +33 (0)1 69 93 50 95 ; Fax: +33 (0)1 69 93 50 44 ;
claire.fargues@agroparistech.fr

ABSTRACT

In order to improve bioethanol production by yeast fermentation of lignocellulosic hydrolysates, sugar/inhibitor separation by nanofiltration was studied on a bench-scale unit equipped with a spiral-wound membrane. Therefore, a model solution containing 3 sugars and 4 inhibitors was treated with two previously selected membranes (NF270 from DOW Filmtec and DK from GE Osmonics). Both membranes led to high sugar rejection, especially at high permeate flux (> 90% for glucose and arabinose and > 85% for xylose). Although its water permeability was smaller, DK membrane was preferred for its higher transmission of the inhibitors, especially for the largest ones (vanillin and 5-hydroxymethyl furfural), ensuring a better detoxification level. Diafiltration was applied to improve sugar purity of the treated hydrolysate. With a diavolume equivalent to 1.25 times that of the feed, acetic acid concentration was divided by 5 and brought back to concentrations lower than 1 g L^{-1}. A simulation model was proposed to predict the diavolume to apply, depending on the initial concentrations. Finally, processed hydrolysates were tested for the fermentation ability with a *Pichia stipitis* species. Fermentation tests showed that diafiltration followed by concentration led to retentates as fermentable as an equivalent pure sugars solution.

1-INTRODUCTION

With advantages of sustainability in comparison with fossil energy sources, bioethanol production is more and more studied for replacing or supplementing the latter. It appears more environmental friendly [1] but with an equivalent-energy 68% lower than that of petroleum [2]. Using by-products of agricultural and forestry industries (lignocellulosic biomass) instead of sugars and corn as initial material is additionally an important breakthrough since it is a very cheap and available resource, presenting no conflict with human food resources [3]. Sugarcane baggasse, rice hull, willow, switch grass, softwood, rice straw, wheat straw, etc. can be used as lignocellulosic biomass for ethanol production with sugar recovery reaching 97% of the original material when cotton was used [4, 5]. However, for most of these available raw materials, fermentable sugar recovery and production of ethanol is more complicated than from starch [6] due to their complex and compact structure including 30 – 50% cellulose, 15 – 35% hemicellulose and 10 – 30% lignin [7]. In most cases, fermentable sugar recovery is rather around 30% of the original material [5] and ethanol production can vary between 1.3 and 95.3 g/L [4] depending on the source and the pretreatment steps. In fact, the process of ethanol production includes several steps, in which acid hydrolysis or pretreatment by acid leads to cellulose destructuration before enzymatic hydrolysis, that releases fermentable sugars [4]. But at the same time, fermentation inhibitors are created, mainly by the degradation of lignins and the dehydration of free sugars. On the one hand, the most common sugars in these hydrolysates are glucose, xylose and arabinose. On the other hand, type and amount of inhibitors depend on the biomass type, pre-treatment and hydrolysis conditions (temperature, pH, etc), but are mainly carboxylic acids, furan derivatives or phenolic compounds. Among them, three major solutes are identified by several authors, whatever the type of the treated biomass and the applied hydrolysis process [8-10]: acetic acid, furfural and 5-hydroxymethyl furfural. Phenolic compounds are generally quantified globally, unless vanillin often appears.

In order to increase fermentation efficiency of those hydrolysates, detoxification methods are currently investigated. They can be physical, chemical, biological or combination of them, each method removing one or some types of inhibitors, rarely all of them. Besides, all of these methods have their own weaknesses. For example, over-liming which consists in alkali addition causes sugar loss [11] and biological detoxification has low efficiency [12]. Among physical treatments, ion exchange and adsorption on resins were first studied [13]. More recently membrane technology gained attention as a cleaner process [14, 15]: it does not

create by-products neither requires chemical addition (in most cases), and is quite straightforward to operate and scale-up. Due to the molecular weights of the solutes to separate (inhibitors molecular weights being inferior to 150 g mol^{-1} when those of sugars are above), membranes such as RO or tight NF of appropriate molecular weight cut-off (MWCO) were studied, especially during the past five years. These studies provide valuable information to target the best membranes to screen: NF90 and NF270 from Dow or DK from GE-Osmonics are often cited, as well as some RO membranes when sugar recovery is preferred to detoxification. But most of them deal with very simple model solutions [16-19] and when more complex or real hydrolysates are considered, dead-end device or very limited flat membrane area are used [20-23].

Before studying and optimizing lignocellulosic hydrolysate detoxification on a bench-scale device (2540 spiral-wound module) and significant filtration area, we conducted a preliminary study on a flat-sheet device with a complex model hydrolysate containing 3 sugars (glucose, xylose and arabinose) and 4 inhibitors (acetic acid, furfural, 5-hydroxymethyl furfural (HMF) and vanillin) [24]. This study, performed with ten NF and RO membranes, led to the selection of two nanofiltration membranes (NF270 – Dow Filmtec (USA) and DK– GE Osmonics (USA)) allowing simultaneously a high transmission of the inhibitors (above 95%) and a very good sugar recovery (between 82 and 95% depending on the sugar). However, even 100% transmitted through the membrane, a solute is still in the retentate at a concentration equivalent to feed concentration. Purification is then expected to occur through concentration mode or diafiltration. Concentration mode leads to the removal of the smallest solutes (inhibitors) in the permeate while the biggest ones (sugars) are rejected and concentrated in the retentate stream, increasing their purity [25, 26]. But doing so, formation of polarization concentration and fouling by accumulation of the rejected species occurs, justifying the choice of diafiltration [16, 20]: during permeate removal, solvent (water) is added to the feed stream to maintain sugars in the retentate at a quite constant concentration while washing out the inhibitors. This method improves the purity of the retentate and ensures an economically acceptable permeation flux. This mode can be continuous or discontinuous and its efficiency depends on the relative rejections, the volume dilution ratio or volume concentration ratio [27, 28]. Eventually, some of the eliminated inhibitors recovered in the permeate, such as furfural, can be valorized depending on their concentration.

The objectives of the present work are to optimize the sugars/inhibitors separation performances at a pre-industrial scale and to estimate the detoxification efficiency by fermentation tests on the purified retentates produced. Therefore, operating parameters

(pressure, feed flow-rate) are studied as well as purification effect through a concentration mode and a diafiltration mode. A solution-diffusion modeling approach is further used to simulate the rejections obtained through diananofiltration.

Sugar sorption on the membranes, highlighted during this study, is also quantified.

2- EXPERIMENTAL

2.1. Model hydrolysate solution and solutes analyses

A solution containing glucose (10 g L^{-1}), xylose (15 g L^{-1}) and arabinose (5 g L^{-1}) as sugars; acetic acid (5 g L^{-1}), HMF (1 g L^{-1}), furfural (0.5 g L^{-1}) and vanillin (0.05 g L^{-1}) as inhibitors, was chosen as model hydrolysate (Table 1). These compounds and concentrations were chosen based on summary of compositions of hydrolysates of various origins [24, 29]. pH of this solution was about 3.

Samples collected during the experiments were analyzed by High Performance Liquid Chromatography (HPLC) on a Betamax Neutral Column (150 mm x 4.6 mm i.d., 5 µm particle size; Thermo-Electron Corporation, Courtaboeuf, France) for inhibitors and a Nucleodur 100-5 NH2-RP column for sugars, as already described in Nguyen et al [24].

Table 1: Model hydrolysate composition and solutes characteristics

Solute	***MW*** **(g mol^{-1})**	**log K_{ow}***	**Concentration (g L^{-1})**
Acetic acid	60	-0.17	5
Furfural	96	0.41	0.5
HMF	126	-0.09	1
Vanillin	152	1.21	0.05
Xylose	150	-1.98	15
Arabinose	150	-2.91	5
Glucose	180	-3.24	10

*: K_{ow} = Partition coefficient of the solute between octanol and water

2.2. Nanofiltration membranes

DK-2540 and NF270-2540 membranes that give best performance in removing inhibitors and retaining sugars were previously selected on a DSS-Labstack M20 device (Alfa Laval, France) [24]. Their characteristics are presented in Table 2. Both membranes are of

semi-aromatic piperazine amide type. As far as we can call “holes” or “pores” the voids in their structure, they have a radius of about 0.4 nm, close to that of some reverse osmosis membranes in the range 0.3 – 0.45 nm [30-32]. Therefore these membranes can be considered as very dense ones.

Table 2: Characteristics of DK-2540 and NF270-2540 membranes

Membrane	**DK2540**	**NF270**
Suppliers	GE Osmonics (USA)	DOW Filmtec (USA)
Molecular Weight Cut Off (MWCO)	150 – 300 [33]	150 – 200 [33] 385 ± 13 [33]
Maximum pressure (bar)	41	41
Maximum temperature (^{o}C)	50	45
Feed-spacer thickness (mil)	30	34
Pore radius (nm)	0.48 ± 0.05 [34] 0.4 – 0.6 [35]	0.34 [36] 0.43 [37]
pH resistance (20 ^{o}C)	2 – 11	3 – 10
$MgSO_4$ retention (%)	98 [33]	> 97 [33]
Isoelectric point (pH)	4.1 [33]	< 3 [33]

2.3. Filtration experiments

Experiments were run at 20 °C on a production bench-scale unit from Polymem (France) equipped with a 2540 spiral-wound membrane (effective membrane area S = 2.6 m^2) (Figure 1). Main parts of the system are made of stainless-steel in order to avoid artifact solute adsorption in the pilot. Pressure probes allow the measurement of inlet and outlet pressures on the feed side, when atmospheric pressure is considered on the permeate side. This pilot plant can be operated in “batch recycling mode” (both permeate and retentate returned to the feed tank) so as to maintain a constant feed concentration, or in “concentration

mode" (retentate recycled back to the feed tank while permeate is removed) in order to increase the Volume Reduction Ratio (*VRR*).

Before treatment on the spiral-wound membrane, each solution was previously micro-filtrated on 10 µm and 3 µm cartridges. For each new condition tested, a 30 min stabilization time was respected before any sampling and measurement. Then permeate flux (J_p) or water flux (J_W) was calculated by permeate flow-rate measurement:

$$J_p, J_W = \frac{v(t)}{S} \qquad (\text{m s}^{-1}, \text{usually expressed in L h}^{-1}\text{ m}^{-2}) \qquad (1)$$

Where $v(t)$ is the permeate flow-rate ($m^3\ s^{-1}$ or $L\ h^{-1}$) and S the effective membrane area (m^2).

Feed, retentate and permeate sampled after stabilization were analyzed by HPLC, allowing the calculation of the rejection of each solute *i*:

$$R_i = \frac{C_{R,i} - C_{P,i}}{C_{R,i}} \qquad (-) \qquad (2)$$

Where $C_{R,i}$ and $C_{P,i}$ are concentrations at retentate side and permeate side respectively ($g\ m^{-3}$). Here, concentration of the feed $C_{F,i}$, ie concentration at the entrance of the filtration module, was considered for $C_{R,i}$.

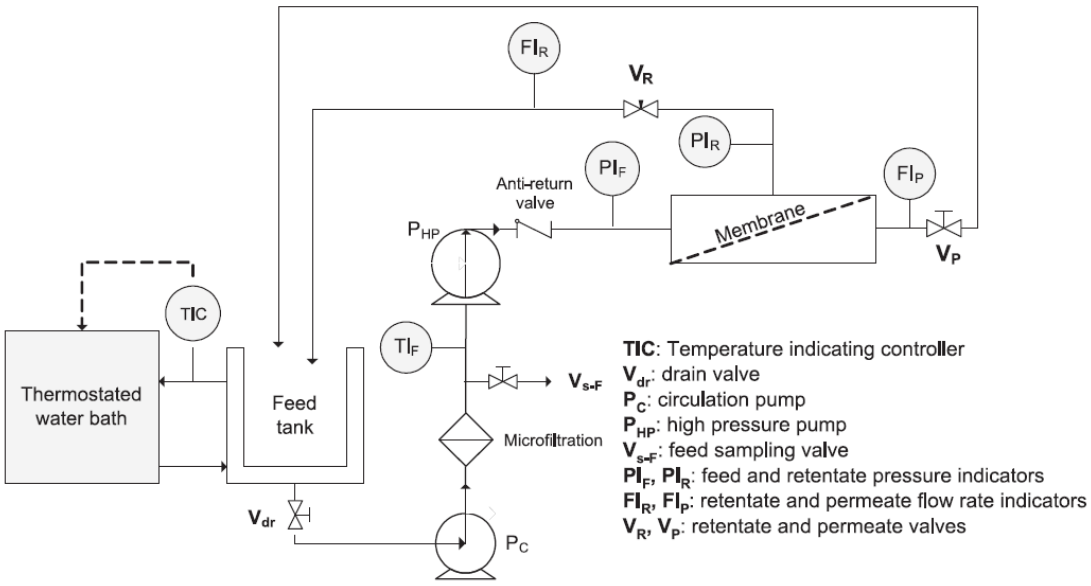

Figure 1. Scheme of the spiral-wound RO bench-scale device (Polymem - France) – Batch recycling mode

For the calculation of the membrane permeability to water, pure water flux was measured at 20 °C, feed flow-rate F_f = 400 L h^{-1} and pressure in the range 5 - 35 bar for DK-2540 and 1 - 6 bar for NF270-2540, due to its much higher water permeability.

Concerning pressure and feed flow-rate optimization, experiments were run in the batch recycling mode with 15 L volume of feed solution. For pressure study, a feed flow-rate of 400 L h^{-1} was used with pressure varying from 5 to 30 bar for DK-2540 and only 4 to 18 bar for NF270-2540.

At the optimized pressures then defined, feed flow-rates from 300 to 600 L h^{-1} were tested for both membranes.

Solution concentration influence on the filtration performances was studied in concentration mode at the optimized pressure and feed flow-rate. A 20 L volume of feed solution was used and concentrated at *VRR* 1, 2, 4 and 8, defined as:

$$VRR = \frac{V_F}{V_F - \sum V_P} \text{ (-)} \qquad (3)$$

Where V_F is the initial feed volume and ΣV_P the total permeate volume extracted till then.

Once the desired *VRR* was reached, a 30 min full recycling mode was run for reaching steady-state, before flow-rate measurement and sampling.

In order to improve inhibitors/sugars separation in the optimized process conditions, constant volume diafiltration was conducted in a discontinuous way, due to a lack of a more adapted equipment: first, a permeate volume equivalent to half the initial feed volume was removed (corresponding to *VRR* 2) at a given permeate flow-rate *v(t)*, then an equivalent volume of water was added. After 30 min stabilization time, flow-rate was measured and samples taken. This procedure or diafiltration step was repeated several times until the inhibitors concentration in retentate was estimated low enough not to cause harm for fermentation microorganisms [38-40]. This discontinuous mode succeeded in simulating the continuous one: calculation of the evolution of C_R through this temporary *VRR* increase (resulting in a temporary increase of $\Delta\Pi$, followed by a decrease of J_P and potential increase of *R*) led to the same C_P evaluation than a continuous calculation (through Eq 12 in part 3.2.).

A purity criterion *P* of the retentates obtained is also calculated as:

$$P = 100 \frac{\sum C_{sugar}}{\sum \left(C_{sugar} + C_{inhibitor} \right)} \quad (\%) \qquad (4)$$

2.4. Evaluation of fermentation ability

Retentates obtained after diafiltration and/or concentration mode were assessed for fermentability (DK membrane only). They were compared with reference solutions (noted **S**) containing similar sugar concentrations but no inhibitors, and with the model hydrolysate.

S. cerevisiae, commonly used for ethanolic fermentation, is unable to convert C5 sugars such as xylose or arabinose. *Pichia stipitis* was therefore chosen for its ability to ferment both C6 and C5 sugars. The selected strain was CBS 5773. It was grown twice for 24 h and 16 h at 28 °C to stationary phase in a Sabouraud broth before being used (pre-culture). Two different fermentation tests were performed: turbidity assays (Bioscreen) and flasks assays.

2.4.1. Turbidimetric assays

The samples were supplemented with $(NH_4)_2SO_4$ 2.5 g L^{-1}; K_2HPO_4 0.3 g L^{-1}; KH_2PO_4 0.5 g L^{-1}; $MgSO_4$ 0.5 g L^{-1} and yeast extract 0.5 g L^{-1} and adjusted to pH 5.5 before sterilization by filtration through a Millipore filter (0.22 µm). They were inoculated with the pre-culture of *P. stipitis* at a final concentration of 10^5 cells mL^{-1} into 3 mL volume. Turbidimetric assays were performed with a Bioscreen C Microbiological Growth Analyser (Labsystems, Helsinki, Finland). Two 100-wells microplates specifically manufactured for this equipment were filled with 200 µL of the different samples. Experiments were run at 28°C. The optical density (OD), linearly correlated to cell concentration, was automatically measured at a 600 nm wavelength every 30 min during a 4 days period. Microplates were shaken 10 s before each measurement in order to avoid yeasts deposit. Data were recorded using the BioLink Dos software provided by the manufacturer and were further analyzed through Microsoft Excel Professional 2007. For each sample, an average value over the corresponding wells was calculated. Standard deviation was 10%. After fermentation, the contents of 5 wells corresponding to the same sample were gathered to allow the analysis of residual sugars.

2.4.2 Flasks assays

Based on Bioscreen results, fermentation of relevant retentates was also carried out through flasks assays at larger time and volume scale ensuring the fermentation process to be completed and concentrations (sugars and ethanol) to be followed over time. Selected samples were supplemented by $(NH_4)_2SO_4$ 5 g L^{-1}, K_2HPO_4 1 g L^{-1}, KH_2PO_4 1 g L^{-1}, $MgSO_4$ 0.5 g L^{-1} and yeast extract 2.5 g L^{-1}, and adjusted to pH 5.5 before sterilization by filtration (0.22 µm). 100 mL of each sample were introduced into a sterile erlenmeyer flask, inoculated at a concentration of 10^6 cells mL^{-1} of yeast culture and then incubated at 25 °C.

Samples were collected twice daily during yeast growth to measure the concentration on a flow cytometer (CyFlow space, Partec, Ste-Geneviève des Bois, France) equipped with a 20-mW 488 nm argon solid state laser. The measurement was performed on Forward Scatter and Side Scatter without staining to obtain the total yeast cells mL^{-1}.

Residual sugars were analyzed at given time intervals (52 h, 70 h, 168 h, 240 h). Ethanol concentration was measured at the end of the experiment (240 h and 2 months) by gas chromatography on an Agilent 6890 plus GC system (Agilent Technologies, Les Ulis, France) equipped with a capillary HP-INNOWax polyethylene glycol (PEG) column (30 m × 530 µm × 1.00 µm) and a FID detector. 1 mL of supernatant culture was transferred to a headspace vial and 20 µL of propanol-1 added as internal standard. Vials were thermostatically controlled for 18 min at 65°C before injection of 500 µL of the volatile phase. Operating conditions were as follows: Helium flow was 8.4 mL min^{-1}, injection temperature 250 °C, detector temperature 240 °C and oven temperature 75 °C. Peak areas were analyzed by Agilent ChemStation software. An ethanol calibration curve was performed from 1 to 40 g L^{-1} to determine the quantity in each sample. All analyses were performed in duplicate.

3- THEORY

3.1. Solution-diffusion modeling

Standard solution-diffusion model [41] is often used to account for non ionic organic solutes transport in dense membranes such as RO and tight NF ones. Considering the voids size of the studied membranes (see par. 2.2), it has been supposed that the transfer mechanism of the non ionized solutes we study would be very close to that with RO membranes, so that SD model could be relevant. This model assumes that both solvent and solute dissolve

partially in the homogenous, non-porous surface layer of the membrane and permeate independently by diffusion under their respective chemical potential gradients. In this model, considering a linear partitioning of the solute between the membrane material and the solution (at retentate and permeate sides), flux $J_{s,i}$ of solute *i* through the membrane is proportional to the difference of solute concentration across the membrane according to:

$$J_{s,i} = \frac{D_{s,i} K_{s,i}}{\delta} \left(C_{R,i} - C_{P,i} \right) = B_i \left(C_{R,i} - C_{P,i} \right) \text{ (gm}^{-2}\text{s}^{-1}\text{)} \quad (5)$$

With:

B_i membrane permeability coefficient to solute i (m s^{-1})

$D_{s,i}$ solute i diffusivity in the polymeric material of the membrane (m^2 s^{-1})

$K_{s,i}$ solute i partition coefficient between membrane and solution (-)

δ active layer (skin) thickness (m)

$J_{s,i}$ can also be defined as

$$J_{s,i} = C_{P,i} J_P \quad (6)$$

Permeate flux is expressed as:

$$J_P = A(\Delta P - \Delta \Pi) \text{ (m s}^{-1} \text{ or L h}^{-1} \text{ m}^{-2}\text{)} \quad (7)$$

With:

A membrane permeability to water (m s^{-1} Pa^{-1}, usually expressed in L h^{-1} m^{-2} bar^{-1})

ΔP hydraulic pressure difference across the membrane (or transmembrane pressure) (Pa)

$\Delta \Pi$ osmotic pressure difference between retentate and permeate (Pa)

Provided solutions are diluted, $\Delta \Pi$ can be deduced by the Van't Hoff relation:

$$\Delta \Pi = RT \sum_{i=1}^{n} \left(c_{R,i} - c_{P,i} \right) \text{ (Pa)} \quad (8)$$

Where $c_{R,i}$ and $c_{P,i}$ are respectively retentate and permeate molar concentrations of solute i (mol m^{-3}).

For experiments with pure water, water flux becomes

$$J_W = A \Delta P \quad (9)$$

and J_W measurement for different ΔP allows A to be calculated.

Combining Eq. 2, 5 and 6 leads to a simple relation between rejection and permeate flux:

$$R_i = \frac{J_P / B_i}{1 + J_P / B_i} \tag{10}$$

For each solute, at different transmembrane pressures (and thus different J_P), minimization between experimental rejections and calculated ones according to Equation 10 allows B_i to be fitted.

Adjusted permeability coefficients A and B_i will further be used to model the diafiltration performances along the successive steps.

3.2. Diafiltration modeling

The mass balance for a diafiltration operation (Figure 2) can be written as follows for each solute i:

$$\frac{dC_{F,i} V_F}{dt} = C_{F,i}\left(v(t) R_i - u(t)\right) \tag{11}$$

Where:

V_F initial feed volume in the tank (m^3)

$u(t)$ diafiltration solvent (water) flow-rate ($m^3\ s^{-1}$)

In a continuous diafiltration mode $v(t)$ and $u(t)$ are set equal and V_F is thus constant. Equation (11) then becomes:

$$\frac{dC_{F,i}}{dt} = \frac{C_{F,i}}{V_F} v(t)\ (R_i - 1) = \frac{C_{F,i}}{V_F} S\ J_P\ (R_i - 1) \tag{12}$$

Where J_P and R_i are predicted according to equations (7) and (10) and to parameters A and B_i estimated from separate experiments. Equations are solved using Matlab R2014a software.

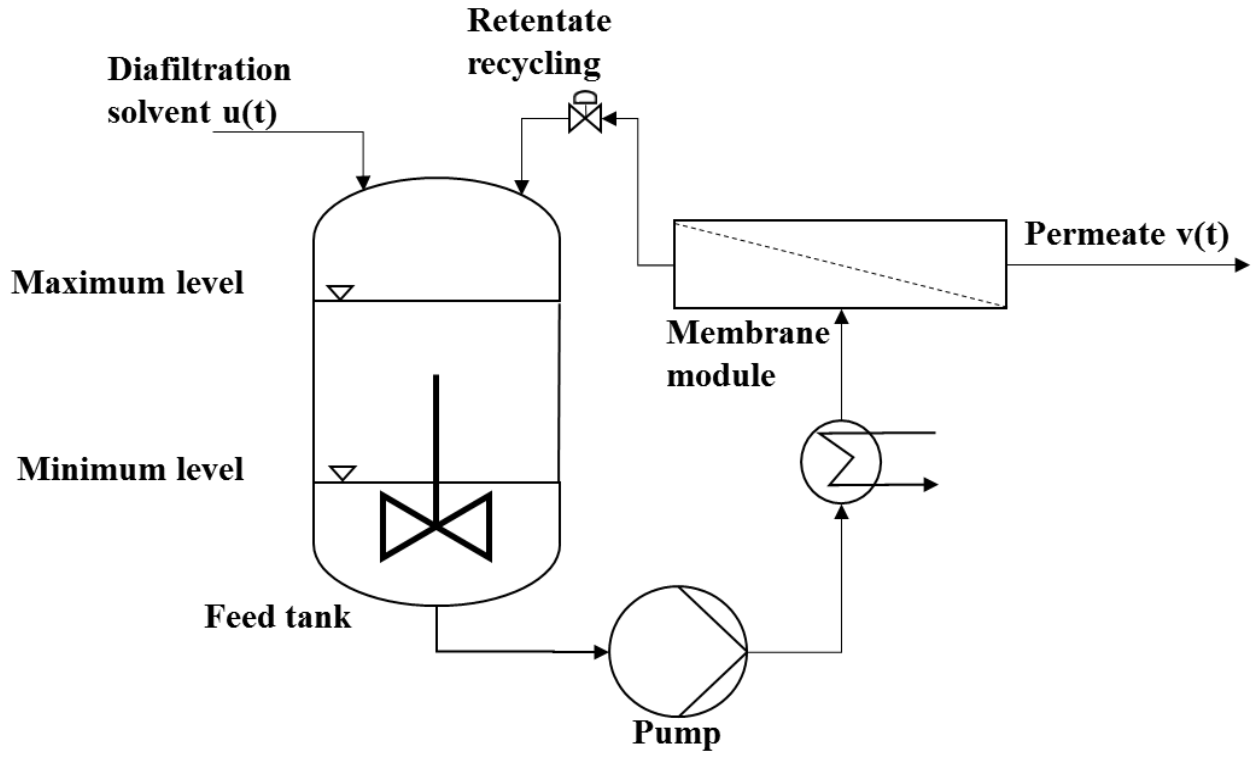

Figure 2. Schematic representation of diafiltration settings

4- RESULTS AND DISCUSSION

4.1. Membrane permeability

Water permeability "*A*" was obtained from J_W measurements for NF270 and DK membranes (Figure 3). Curves are linear following equation 9 and lead to A= 8.6 L h^{-1} m^{-2} bar^{-1} for NF270 and A = 3.3 L h^{-1} m^{-2} bar^{-1} for DK, which is 30% and 45% less than that obtained through flat-sheet experiments on a DSS-Labstack device [24]. Influence of filtration equipment geometry on water permeability had already been pointed out by several authors [42, 43] and attributed to a lower flow velocity and smaller membrane elasticity in spiral-wound modules, or to a higher proportion of unexploited membrane area. Concerning the geometry differences, the space provided in the plate and frame system used in Nguyen et al [24] is delimited by two superimposed circular surfaces (the membrane and the frame). The liquid flows from the centre to the outer edge, and the retentate velocity for a flow-rate of 400 L h^{-1} would be about 1 m s^{-1} depending on the radial position. In the spiral wound membrane (2540 module), taking account of spacer thickness, the retentate velocity is much smaller at

about 0.1 m s^{-1}. This confirms the relevance of studying such process at the pre-industrial scale.

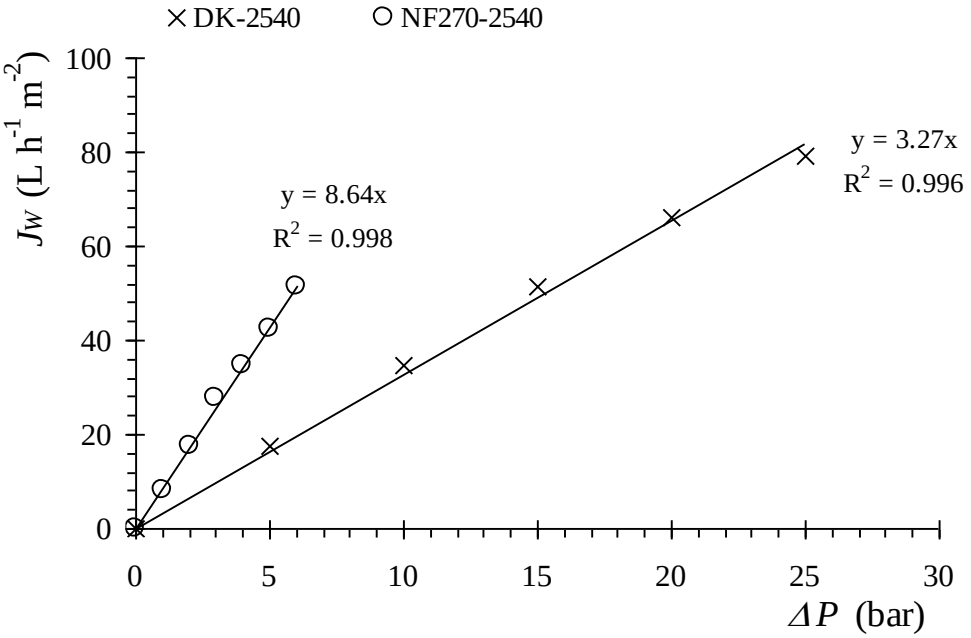

Figure 3. Pure water flux study (F_f = 400 L h^{-1}; T = 20°C).

4.2. Optimization of filtration parameters

Rejection results obtained for inhibitors and sugars for different pressures ΔP are given in Figure 4. Solution-diffusion model was tested and B_i coefficients calculated according to equation (10) by a non-linear minimization method (Table 3). For NF270, only permeate fluxes below 40 L h^{-1} m^{-2} were considered. In fact, for sugars, a further ΔP increase did not lead to an improvement of the rejection, showing that this model was not relevant anymore. It is probably due to coupled solutes transfer or to the formation of a polarization concentration layer that was not taken into account in the model. However, modeling tendency with B_i adjusted that way seems to be convenient for inhibitors rejection at most pressures (Figure 4). Except for acetic acid, permeability of DK membrane for sugars and inhibitors is similar or higher to that of NF270. It even leads to a negative rejection for furfural corresponding to an infinite permeability. In order to avoid clutter, simulations for DK are not shown in Figure 4.

As already noticed in the screening study [24], except for vanillin, inhibitors transmission is similar for both membranes: about 100% for furfural, 98% for acetic acid, and above 94% for HMF whatever the pressure (Figure 4a). DK membrane leads to a smaller vanillin rejection (or a higher transmission) than NF270. Simultaneously, glucose rejection is quite the same for both membranes (Figure 4b) which is an important point, as glucose is the easiest fermentable sugar. As in [24], rejection order for sugars is unchanged, with $R_{glucose} > R_{arabinose} > R_{xylose}$, arabinose being better rejected than xylose due to its higher hydration number as already discussed. When results are similar between flat-sheet and spiral-wound geometries concerning the inhibitors and glucose, a difference arises for C5 sugars: rejection of xylose and arabinose is improved of at least 12 % for NF270 at spiral-wound scale (for equivalent permeate flux) whereas it is quite unchanged for DK. Being intermediate, C5 sugars rejection (as that of vanillin) is certainly more sensitive to feed hydrodynamics. It should be noted that feed spacer geometry of spiral-wound modules is different for both suppliers: 34-mil for NF270 (DOW Filmtec), designed to lessen the fouling, and 30-mil for DK (GE Osmonics). Again, this highlights the importance of studying separation at spiral-wound scale.

Table 3. Permeability coefficient B_i of NF270 and DK membranes for inhibitors and sugars according to solution-diffusion model (Equation 10)

Solute	Acetic acid	Furfural	HMF	Vanillin	Xylose	Arabinose	Glucose
NF270 - B_i ($m\ s^{-1}$)	$2.9.\ 10^{-4}$	$2.5.\ 10^{-3}$	$1.1.10^{-4}$	$4.9.\ 10^{-5}$	$8.5.\ 10^{-7}$	$4.5.\ 10^{-7}$	$1.8.10^{-7}$
DK - B_i ($m\ s^{-1}$)	$2.6.\ 10^{-4}$	-	$9.0.10^{-5}$	$5.9.\ 10^{-5}$	$1.0.\ 10^{-6}$	$7.6.\ 10^{-7}$	$1.7.10^{-7}$

a) Inhibitors

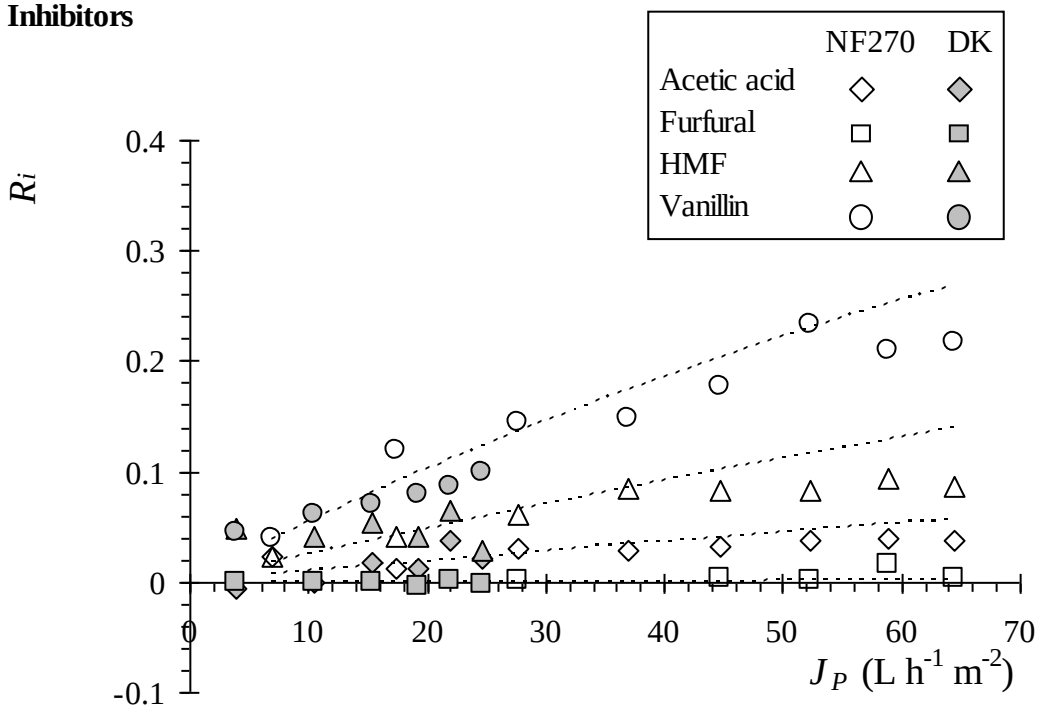

b) Sugars

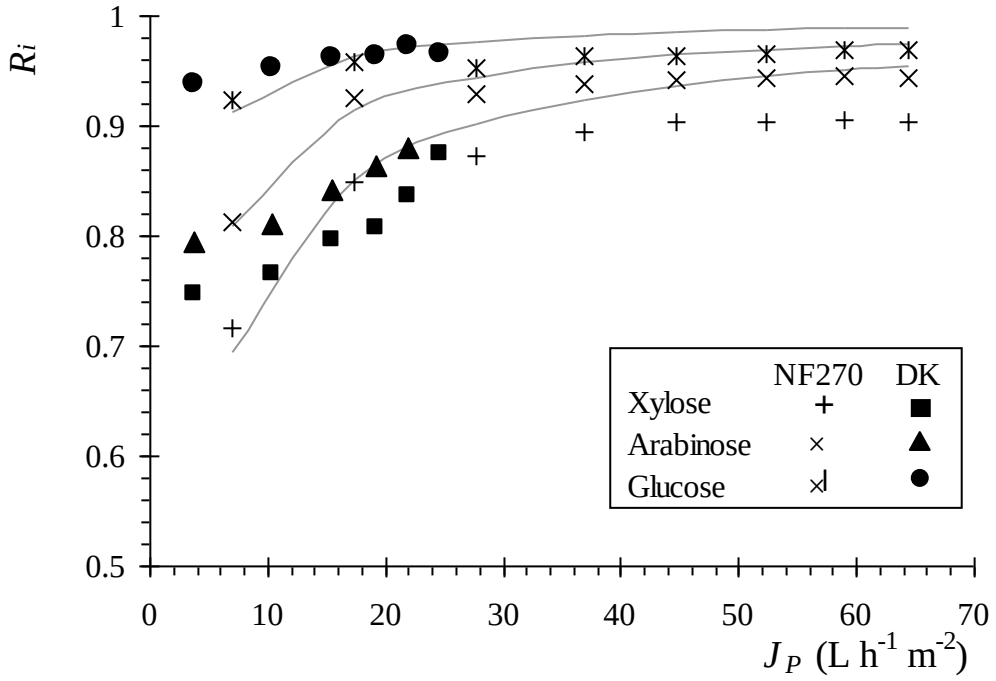

Figure 4. Effect of pressure on solutes rejection: a) Inhibitors; b) Sugars.

Lines correspond to modeling for NF270 results according to Equation 10; (F_f = 400 L h^{-1}; T = 20°C; ΔP = 4, 6, 8, 10, 12, 14, 16 and 18 bar for NF270; ΔP = 5, 10, 15, 20, 25 bar for DK).

Glucose rejection is very high with NF270 and quite independent of pressure, whereas it varies for C5 sugars which are partially rejected. Consequently, a cut-off between 150 and 160 g mol^{-1} may be assessed for this membrane: solutes with larger *MW* should always be well rejected (as C6 sugars) due to the predominance of steric hindrance in the rejection mechanism. Rejection difference between C5 sugars and vanillin of equal molecular weight (about 150 g mol^{-1}) highlights the fact that for solutes with *MW* in the range of the MWCO, affinity and interactions with the membrane material have a deep impact on the rejection. Vanillin probably interacts through π–π interactions with the active layer of the membrane, when C5 sugars, more hydrated and interacting less, are rejected [24]. For DK membrane the cut-off is probably higher, above 160 g mol^{-1}, explaining vanillin higher transmission. This is consistent with the larger pores of this latter membrane (Table 2). Using DK membrane would then correspond to a better detoxification of the retentate (relatively to vanillin, the biggest inhibitor better transmitted) but to a higher loss of C5 sugars.

Fluxes are much higher with NF270 membrane which leads to a sugar rejection plateau at lower ΔP than DK. Consequently, pressures of 10 bar and 15 bar were chosen respectively for NF270 and DK membranes for further experiments, leading to J_P = 35 L h^{-1} m^{-2} for NF270 and J_P = 15 L h^{-1} m^{-2} for DK. Again, these values are much smaller than those obtained previously with the model solution on the plate and frame device (membrane selection [24]), which is consistent with the smallest permeability underlined sooner for spiral-wound geometry: for the same pressure conditions of 10 and 15 bar respectively, permeate fluxes were about 65 L h^{-1} m^{-2} for both membranes.

Feed flow-rate (F_f) increase improves inhibitors and sugars rejection at varying degrees depending on the membrane (Figure 5). This can be explained by a decrease of the laminar hydrodynamic layer thickness where concentration polarization takes place [44]: it would lead to an increase of the effective transmembrane pressure following $\Delta \Pi$ decrease [45, 46]. For DK membrane, acetic acid and furfural transmission through the membrane is quite total whatever the flow-rate. For other inhibitors or with NF270, rejection increase is limited: from 15% to 23% for vanillin with NF270 against 4.5% to 10% with DK. Flow-rate influence on pentose's rejection is again much sensitive with DK membrane. For DK it seems then essential to process with the highest feed flow-rate in order to recover as much sugar as possible in the retentate. The value of 600 L h^{-1} was thus chosen for the following experiments.

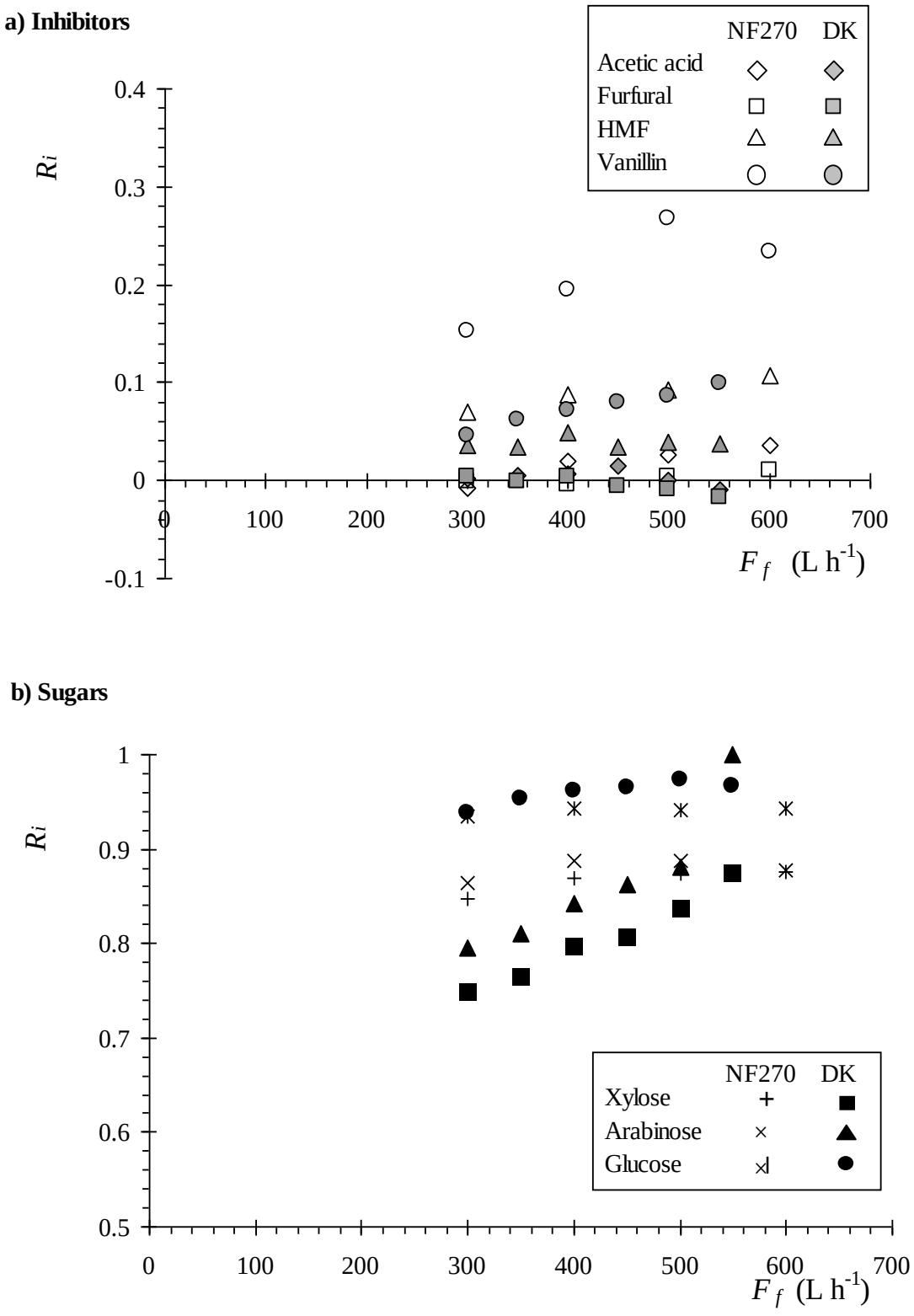

Figure 5. Effect of feed flow-rate on solutes rejection: a) Inhibitors ; b) Sugars.
(T= 20 °C; ΔP= 10 bar for NF270; ΔP = 15 bar for DK)

4.3. Concentration mode and diananofiltration study for an improvement of sugars purity

4.3.1. Concentration mode study

Concentration mode was studied at the optimized feed flow-rate of 600 L h^{-1} and a ΔP of 10 bar for NF270 and 15 bar for DK. It aims to improve the -sugars to inhibitors- ratio in the concentrated retentate, leading to a better fermentation requirement. As the applied ΔP is maintained constant during the experiments, *VRR* increase leads to an important decrease of the permeate flux as shown in Figure 6: from 33.8 to 3.2 L m^{-2} h^{-1} for NF270 for a *VRR* increase from 1 to 4 (it was not possible to achieve higher *VRR* in that case) and from 19.8 to 4.6 L m^{-2} h^{-1} for DK membrane for a *VRR* increase from 1 to 8. This was ascribed to the evolution of the osmotic pressure caused by sugars rejection: for *VRR*4, concentration of sugars leads to a calculated $\Delta\Pi$ of 8.4 bar when it was 3.7 bar at *VRR*1. A decrease of the rejection for all the solutes is noticed simultaneously, especially for the highly transmitted inhibitors until giving negative rejections even for NF270 (Figure 6a). It is well known that rejection evolves alongside with water flux. But apart from this influence, decrease of acetic acid rejection in presence of sugar had already been noticed by several authors [17, 47]. It could be attributed to a dehydration effect of the less polar solutes (the inhibitors) due to the concentration increase of highly polar ones (sugars) that monopolize water molecules (according to log K_{OW} values, Table 1). At the same time and as already noticed in Figure 4, sugars rejection decrease is limited at about 5% whatever the flux due to their high rejection (Figure 6b). As expected, sugars purity criterion (Eq. 4) increases with *VRR* (Table 4), due to the concentration effect on sugars in the retentate and inhibitors composition stability. Both membranes give similar results with a purity increase of around 8% from *VRR*1 to 4, which reaches 10% for *VRR*8 (DK membrane), sugars optimal purity being then about 94%.

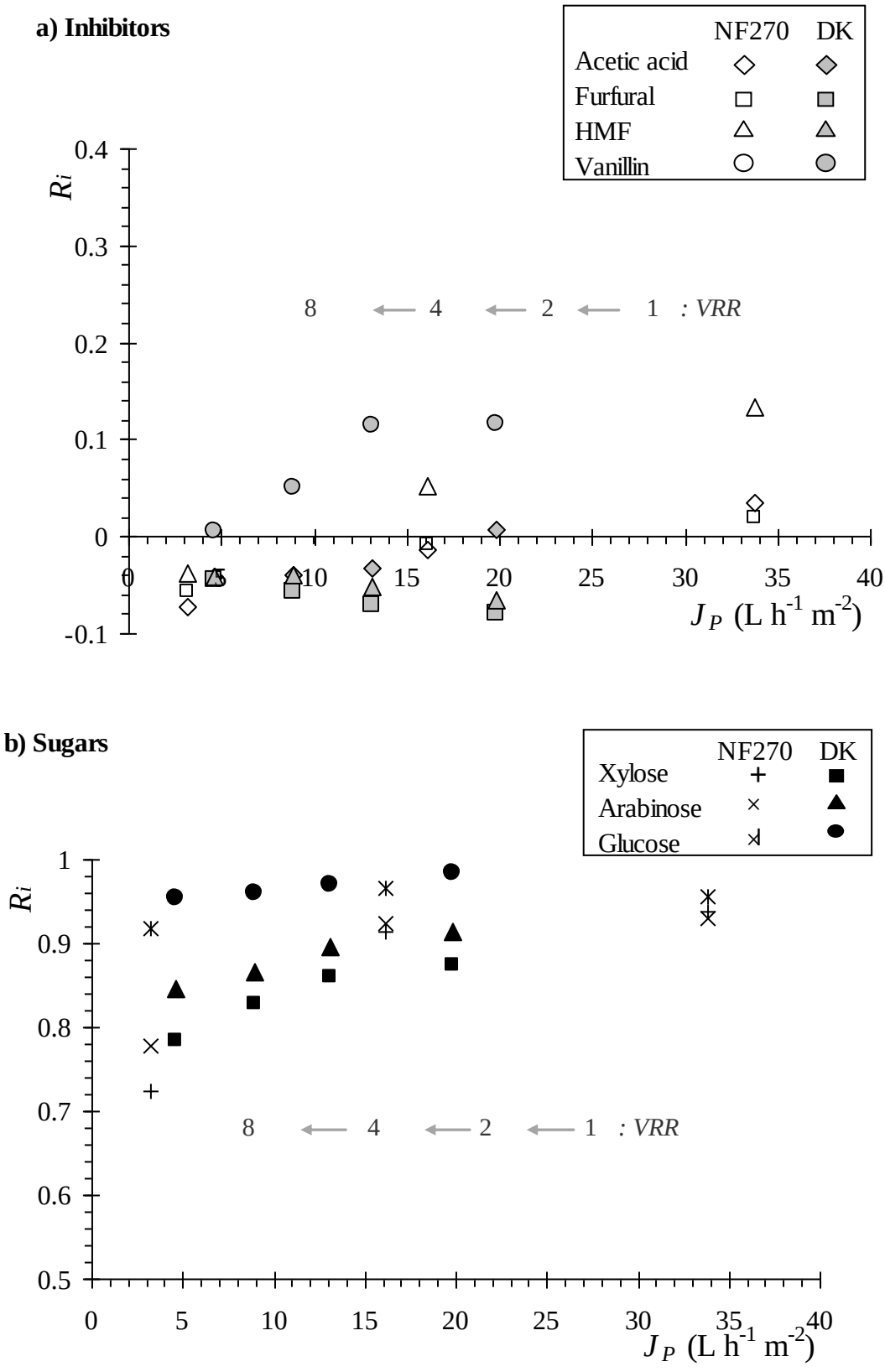

Figure 6. Effect of *VRR* increase on solutes rejection: a) Inhibitors; b) Sugars.
(F_f = 600 L h^{-1}; T = 20°C; ΔP = 10 bar and *VRR* = 1, 2, 4 for NF270; ΔP = 15 bar and *VRR* = 1, 2, 4, 8 for DK).

Table 4. Retentate composition and purity criterion evolution (Eq. 4) through concentration mode, for both membranes tested

		NF270			DK			
Solution type	Feed	*VRR*1	*VRR* 2	*VRR* 4	*VRR* 1	*VRR* 2	*VRR* 4	*VRR* 8
Concentration (g L^{-1})								
Acetic acid	5.02	5.32	5.32	5.24	3.96	4.60	3.93	3.74
Furfural	0.52	0.41	0.40	0.38	0.66	0.77	0.62	0.59
HMF	0.98	0.89	0.92	0.91	0.65	0.79	0.66	0.64
Vanillin	0.046	0.046	0.051	0.049	0.052	0.063	0.053	0.054
Xylose	15.4	15.7	24.2	36.0	13.4	23.5	27.9	35.6
Arabinose	5.76	6.54	7.85	12.4	6.13	9.17	11.2	14.8
Glucose	10.22	12.1	15.4	24.6	9.66	18.3	23.6	31.5
Solution purity criterion *P* (%)								
	82	84	88	92	85	89	92	94

Table 4 also shows that *VRR* increase is not followed by a proportional increase of sugars concentration, even for sugars rejected at more than 95%. Mass balance calculations from one *VRR* to the following highlight a loss of at least 10% of the sugar quantity initially present in the system and that whatever the sugar. Concentration from *VRR*1 to 8 with DK membrane leads to an overall loss of sugar above 50%. Such a gap between experimental and expected concentration factors when increasing *VRR* is noticeable in similar studies [19, 22, 48], even though authors do not emphasize it. In order to quantify and understand this phenomenon, sorption tests were run in the equipment: a given volume of a mono-component solution of glucose (as reference) of known initial concentration was circulated in the spiral-wound pilot in full recycling mode (at 20°C, feed flow rate of 600 L h^{-1} and no pressure applied). Main parts of the pilot being in stainless steel (even the pressure vessel elements), artifact adsorption was considered as negligible. Measurement of the initial and equilibrium glucose concentration in the feed associated to a mass balance on the system gives the adsorbed quantity q (g m^{-2}) on the membrane, in equilibrium with the remaining concentration C in solution. Different initial concentrations of glucose were investigated that way, which allowed sorption isotherm to be drawn. Dilution of the more concentrated glucose solution

studied in the pilot plant was also investigated in order to test sugar desorption from membrane surface and appreciate the sorption reversibility. The resulting sorption isotherm on both investigated membranes is shown in Figure 7.

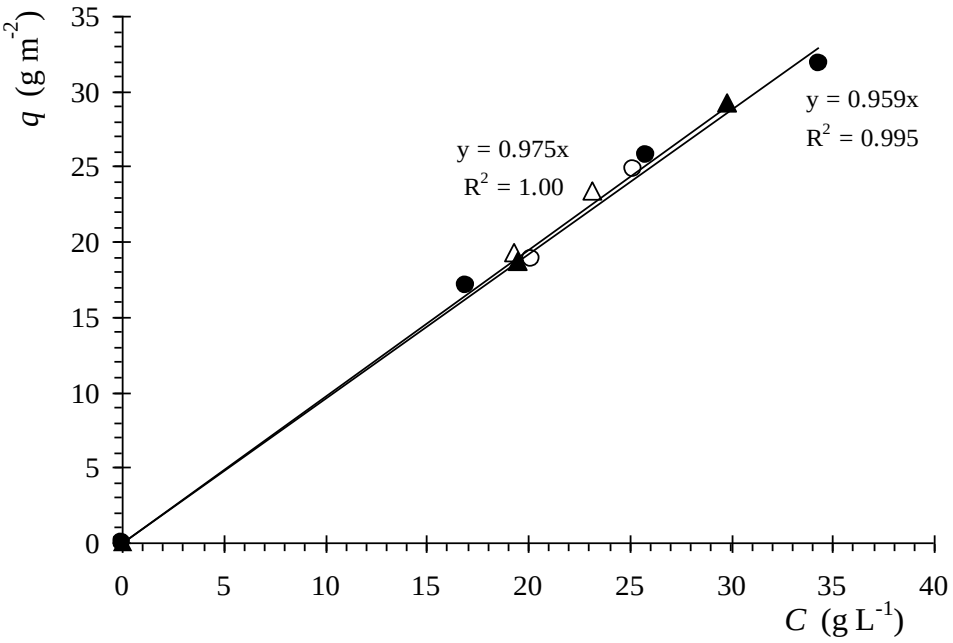

Figure 7. Glucose sorption isotherm for DK membrane (● sorption; ○ Desorption) and NF270 membrane (▲sorption; Δ Desorption).

As suggested, an important quantity of glucose is fixed on the membrane which explains the "disappearance" from the whole system during filtration experiments: for a membrane surface of about 2.5 m^2 and glucose concentration about 20 g L^{-1}, the sorbed quantity would be of 20 g m^{-2} according to those measurements, indicating that 50 g of glucose are either adsorbed or trapped in the membrane material. However, the performed experiments do not make it possible to distinguish between ad- or ab-sorption. Both membranes give the same result, and desorption tests show that it is a reversible process as the points are perfectly superimposed with sorption ones. Glucose sorption appears clearly to be a linear partitioning between the solution and the membrane in the concentration range tested (up to 35 g L^{-1}). An average partition coefficient can then be calculated as

$$a = q/C = 0.97 \text{ (L m}^{-2}\text{)} \quad (13)$$

q being the sorbed amount of glucose (g m^{-2}) and C its equilibrium concentration in solution (g L^{-1}).

Bioscreen test was run on the model hydrolysate and the retentates obtained at *VRR*=1, 2, 4, 8 with DK membrane and compared with reference solutions S1, S2 and S3 containing sugars only (Table 5). Comparing model hydrolysate with S1 shows that inhibitors significantly delay yeast growth with lag time increased from 5 to 50 h (Figure 8). With retentates from *VRR* 1 to 8, yeast growth could hardly be seen in the course of the experiment whereas S2 and S3 displayed growth curves quite superimposed to S1. Sugars analyses confirm a strong adverse effect of inhibitors on retentates, with no sugar consumed within the experiment (100 h), whereas 100%, 83% and 25% glucose was consumed in S1, S2 and S3, respectively. Xylose was partially consumed in S1 only (24%). Results indicate that *P. stipitis* CBS 5773 consumes xylose only when glucose is depleted. Arabinose was not consumed within this experiment. In the case of *VRR*8 experiment and unlike for V*RR*1, 2 and 4, cell growth starts after 75h. This burst of growth may not be significant; hypothetical metabolic adaptation of *P. stipitis* cells to the presence of inhibitors promoted by higher concentrations in sugars (see Table 4) may be advanced.

Purification of the hydrolysate through sugars concentration (nanofiltration in a concentration mode) is clearly not the good strategy, as it is not followed by an improvement of the retentate fermentability. On the contrary, the slight increase of the concentration of some partially transmitted inhibitors, namely vanillin and furfural, seems to have a very negative impact on the fermentability. Actually, vanillin and furfural are pointed out in different studies to be especially severe inhibitors [49, 50].

Table 5. Reference sugars solutions tested for fermentation (to be compared to Table 4)

Reference solution	Concentration (g L^{-1})		
	Glucose	Xylose	Arabinose
S1	10.0	15.0	5.0
S2	20.0	25.0	10.0
S3	30.0	35.0	15.0
S4	30.0	28.0	12.0

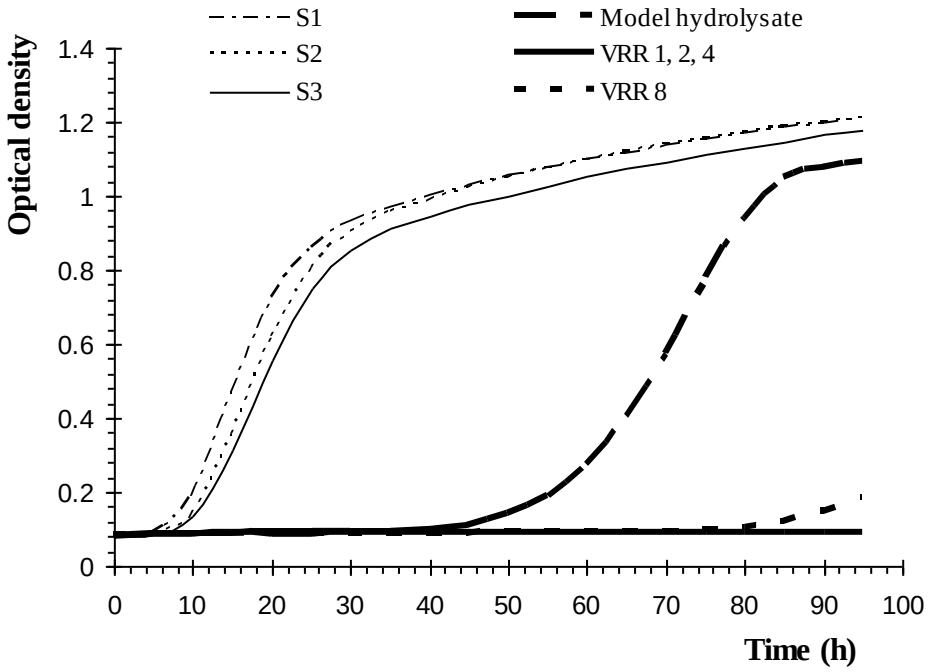

Figure 8. Yeast growth study by turbidimetric assays (Bioscreen) on retentates obtained by nanofiltration in a concentration mode (DK membrane)

4.3.2. Diananofiltration study

Constant volume diafiltration mode was run in a discontinuous way in order to remove the inhibitors from the retentate until concentration levels ensuring satisfactory fermentation results. Better than a dilution of the inhibitors, the addition of water is expected to limit the formation of the concentration polarization layer on membrane's surface. It decreases the eventual pores clogging, facilitating the transport of small solutes through the membrane. As expected, inhibitors concentration gradually decreases with diafiltration step (Figure 9a). With NF270, after 3 steps (Diavolume/V_F = 1.5), acetic acid concentration is below 1 g L^{-1} (0.78 g L^{-1}), that of HMF, furfural and vanillin being 0.21, 0.09 and 0.013 g L^{-1}, respectively. Sugars concentration also decreases (Figure 9b) but in a lower extent due to their high rejection: xylose concentration decreases from 14.4 to 13.4 g L^{-1} after 3 steps, when arabinose stays quite constant at about 4.5 g L^{-1} as well as glucose at about 9.7 g L^{-1}. Results are similar for the inhibitors with DK membrane, but loss of sugars in permeate is faster leading to a lower recovery in the retentate. This is explained by their smaller rejection as already noticed when optimizing pressure and feed flow-rate, the highest loss being about 20% for xylose. For glucose, it remains moderate at 8%, compared to only 2% with NF270 membrane. Through

diafiltration, purity criterion is improved significantly: it reaches 98% for NF270 and 99.9% for DK after five steps, instead of 92% for the former (for *VRR*4) and 94% for the latter (for *VRR*8) in the concentration mode. Diafiltration proves efficient to remove the inhibitors at the cost of a small sugar loss however (especially for DK membrane). Figure 9 also shows a very good fitting of the simulated C_F with experimental results for NF270. Successful modeling of diafiltration is useful to predict the amount of water needed to "wash" the hydrolysate until reaching acceptable concentrations of different inhibitors, suitable for fermentation. As an example, a 1 g L^{-1} threshold for acetic acid (the most concentrated inhibitor) would be reached with NF270 membrane with a water volume equal to 1.25 times the feed volume.

On this basis, 3 steps of diafiltration were run with DK membrane (Diavolume/V_F = 1.5) and the diafiltrated AD retentate was tested for fermentability. Bioscreen test displayed lag phase and growth rate close to S1 showing that inhibitors concentration (Table 6) was reduced enough to allow yeasts to grow in the best conditions. At the end of the Bioscreen test, 100% of glucose and 60% of xylose were converted. Based on these results, the diafiltrated retentate AD was further concentrated at pilot scale to *VRR* 8 (ADC8): indeed, many authors showed that increasing initial sugar concentration up to 100 – 110 g L^{-1} leads to an improvement of fermentation performances [51, 52]. Through the concentration step, purity criterion evolves from 95.4% for AD to 98.6% for ADC8. Fermentation in flasks was run for both AD and ADC8 retentates and compared to the untreated model hydrolysate and the relevant reference sugar solutions S1 and S4. Fermentation of ADC8 displays no lag phase and growth rate is similar to AD, S1 and S4 (Figure 10). However, the growth of cells stabilizes after 50h fermentation, reaching the stationary phase at a value equivalent to the model hydrolysate but lower than AD, S1 and S4. Regarding sugars conversion, performances for ADC8 are at least equivalent to S4 and even better with 29% xylose converted instead of 13% for S4 at the end of the experiment (240h). 100% glucose was converted in both cases.

Table 6. Composition of the retentates obtained by diafiltration with DK membrane

Samples	Concentration (g L^{-1})						
	Glucose	Xylose	Arabinose	Acetic acid	Furfural	HMF	Vanillin
Diafiltrated retentate (AD)	7.92	10.32	4.07	0.832	0.079	0.151	0.006
Diafiltrated and concentrated retentate (ADC8)	29.11	28.35	12.17	0.784	0.077	0.154	0.007

a) Inhibitors

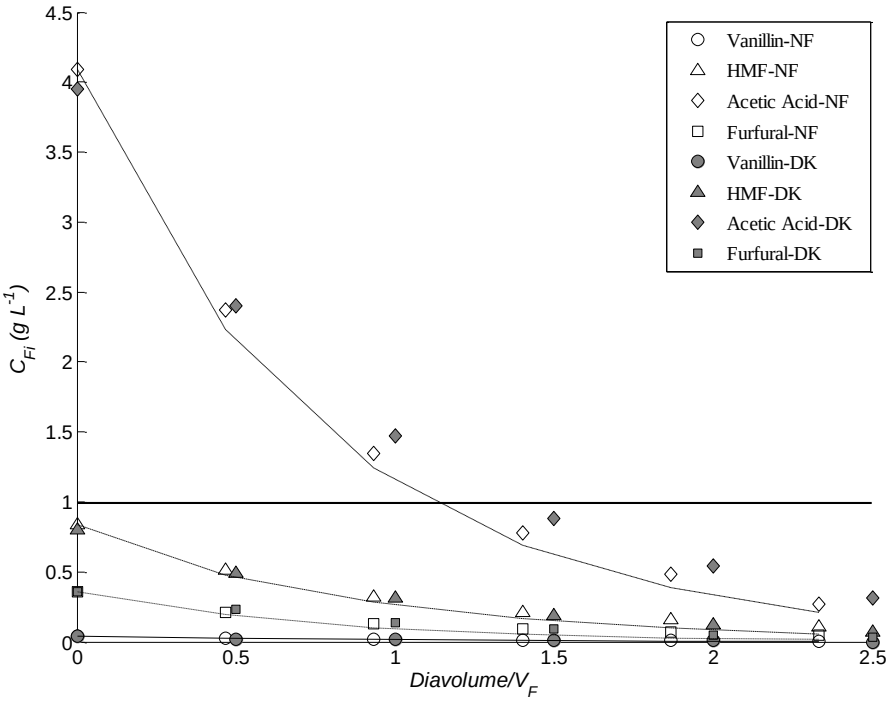

b) Sugars

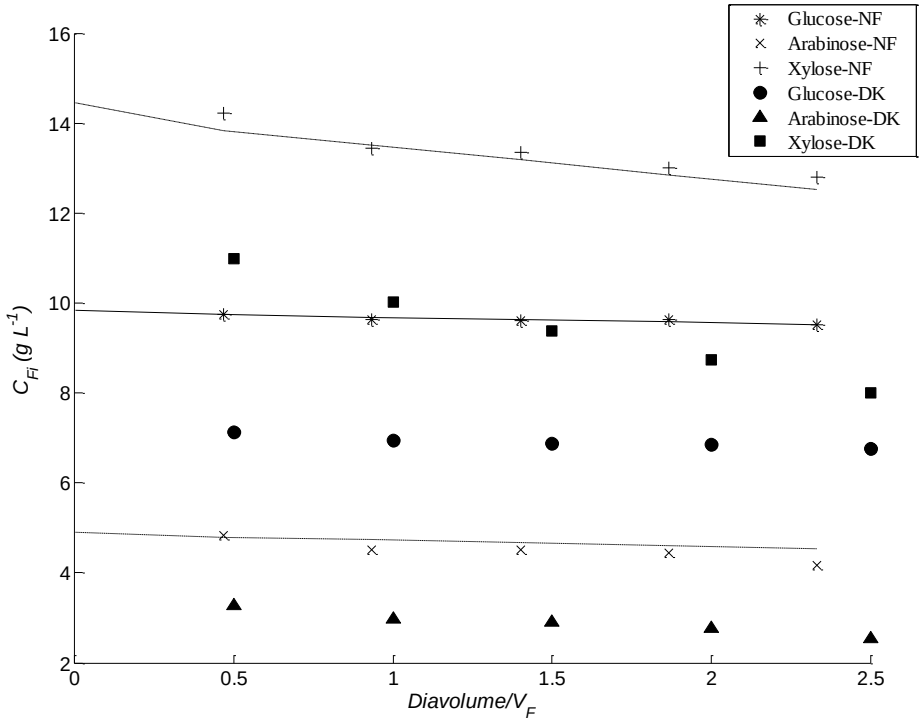

Figure 9. Feed concentration modification during diafiltration with NF270 and DK membranes: a) Inhibitors; b) Sugars.

Lines represent modeling for NF270 according to equation (12).

(F_f = 600 L h^{-1}; T = 20°C; ΔP = 10 bar for NF270; ΔP = 15 bar for DK)

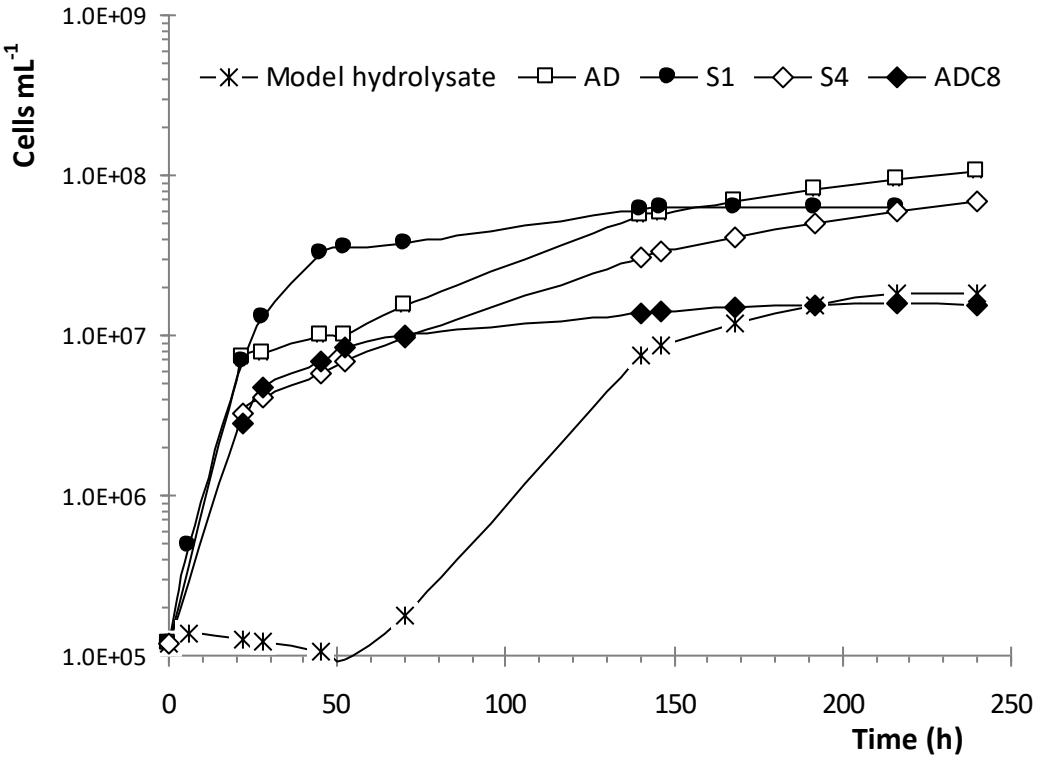

Figure 10. Yeast growth study with flask assays on retentates obtained by nanofiltration in a diafiltration mode before (AD) and after (ADC8) concentration (DK membrane)

Fermentation yield was calculated as the ratio between the concentration of produced ethanol and the initial concentration of fermentable sugars, here [glucose + xylose]. Arabinose was not considered as it could not be converted by *P. stipitis*. For *S. cerevisiae* grown on glucose, the theoretical yield is 0.51; in practice, it never exceeds 0.49. Regarding *P. stipitis* grown on glucose, the yield is known to be more or less equivalent, but for xylose conversion, it is around 0.3 depending on the fermentation conditions [53]. Therefore, provided that xylose is fully converted, we can expect a global yield between 0.3 and 0.49 depending on xylose ratio in the samples. From ethanol concentrations at 240 h and after 2 months, it is observed that fermentation is not completed within 240 h (Table 7); this is especially visible for samples with high sugar concentrations (S4 and ADC8). Yields obtained after 2 months are between 0.19 and 0.25, which is lower than expected, probably due to non optimized growth conditions (uncontrolled aeration, for example) and to the choice of the strain. However, the highest yield is achieved for ADC8, equivalent to S4 and better than model hydrolysate, S1 and AD.

Table 7. Ethanol concentration after 240 h and 2 months in flasks assays and fermentation yield

Samples	EtOH concentration (g L^{-1})		Initial [glucose+xylose] (g L^{-1})	Yield*
	240 h	2 months		
AD (Diafiltrated retentate)	3.24	3.57	18.23	0.20
ADC8 (Diafiltrated and concentrated retentate)	11.79	14.11	57.46	0.25
Model hydrolysate	4.35	4.91	25.62	0.19
S1	4.82	4.65	25.00	0.19
S4	10.73	14.60	58.00	0.25

* calculated from ethanol concentration after 2 months

CONCLUSION

From a screening study at a small flat-sheet scale, two nanofiltration membranes (NF270 and DK membranes) proved to be efficient for the separation of sugars (C5 and C6) from fermentation inhibitors of similar molecular weights [24]. The pre-industrial scale process on 25-40 spiral-wound modules for each membrane was optimized. NF270 membrane could be used at lower transmembrane pressures due to its higher water permeability. Both membranes showed comparable rejection results for glucose, when smaller rejection was obtained for C5 sugars in the case of DK membrane (5% less in the worst cases). Simultaneously, smaller rejection and then higher transmission of the biggest inhibitors was obtained with this membrane (vanillin was up to 15% more transmitted), ensuring a better detoxification result for an equivalent sugar recovery. DK membrane was thus preferred. For both membranes, diananofiltration was studied and led to an improvement of sugar purity up to a factor 1.2 as compared to the initial hydrolysate in the case of DK membrane, corresponding to a sugar purity criterion close to 100%. On the basis of diafiltration modeling results, diafiltration was run on the hydrolysate until a 1.5 feed volume level, allowing inhibitors concentration to decrease below a conjectured critical level, especially for acetic acid content. It was followed by a concentration step in order to further enhance the sugar purity. In fermentation, the resulting detoxified hydrolysate showed a cell growth equivalent to that of a pure sugar solution of similar concentration, as well as a good glucose conversion yield into ethanol. This confirmed its harmlessness for the yeasts used in this case.

These results encourage coupling fermentation systems to membrane processes to improve bioethanol production yields.

Acknowledgments

This work is part of Dr. D. T. N. N. Nguyen doctorate thesis. Vietnam International Education Development (VIED) is acknowledged for contributing financially to her stay in France.

References

[1] M. Cantarella, L. Cantarella, A. Gallifuico, A. Spera, F. Alfani, Comparison of different detoxification methods for steam-exploded poplar wood as a substrate for the bioproduction of ethanol in SHF and SSF, Process Biochem. 39 (2004) 1533-1542.

[2] S.I. Mussatto, G. Dragone, P.M.R. Guimaraes, J.P.A. Silva, L.M. Carneiro, I.C. Roberto, A. Vicente, L. Domingues, J.A. Teixeira, Technological trends, global market, and challenges of bio-ethanol production, Biotechnol. Adv. 28 (2010) 817-830.

[3] R.E.H. Sims, W. Mabee, J.N. Saddler, M. Taylor, An overview of second generation biofuel technologies, Bioresource Technology 101 (2010) 1570-1580.

[4] R. Singh, A. Shukla, S. Tiwari, M. Srivastava, A review on delignification of lignocellulosic biomass for enhancement of ethanol production potential, Renew. Sust. Energ. Rev. 32 (2014) 713-728.

[5] L. Vallander, K.-E.L. Eriksson, Production of ethanol from lignocellulosic materials: state of the art, in Bioprocesses and Applied Enzymology, A. Fiechter, Editor. 1990, Springer Berlin Heidelberg. p. 63-95.

[6] K. Öhgren, R. Bura, G. Lesnicki, J. Saddler, G. Zacchi, A comparison between simultaneous saccharification and fermentation and separate hydrolysis and fermentation using steam-pretreated corn stover, Process Biochem.42 (2007) 834-839.

[7] L.D. Sousa, S.P.S. Chundawat, V. Balan, B.E. Dale, 'Cradle-to-grave' assessment of existing lignocellulose pretreatment technologies, Curr. Opin. Biotechnol. 20 (2009) 339-347.

[8] S.I. Mussatto, I.C. Roberto, Alternatives for detoxification of diluted-acid lignocellulosic hydrolyzates for use in fermentative processes: a review, Bioresource Technol. 93 (2004) 1-10.

[9] N.N. Nichols, B.S. Dien, M.A. Cotta, Fermentation of bioenergy crops into ethanol using biological abatement for removal of inhibitors, Bioresource Technol. 101 (2010) 7545-7550.

[10] T. Sainio, I. Turku, J. Heinonen, Adsorptive removal of fermentation inhibitors from concentrated acid hydrolyzates of lignocellulosic biomass, Bioresource Technol. 102 (2011) 6048-6057.

[11] E.W. Jennings, D.J. Schell, Conditioning of dilute-acid pretreated corn stover hydrolysate liquors by treatment with lime or ammonium hydroxide to improve conversion of sugars to ethanol, Bioresource Technol. 102 (2011) 1240-1245.

[12] W. Parawira, M. Tekere, Biotechnological strategies to overcome inhibitors in lignocellulose hydrolysates for ethanol production: review, Crit. Rev. Biotechnol. 31 (2011) 20-31.

[13] N.O. Nilvebrant, A. Reimann, S. Larsson, L.J. Jönsson, Detoxification of lignocellulose hydrolysates with ion-exchange resins, Appl. biochem. biotech. 91-93 (2001) 35-49.

[14] C. Abels, F. Carstensen, M. Wessling, Membrane processes in biorefinery applications, J. Membrane Sci. 444 (2013) 285-317.
[15] Y. He, D.M. Bagley, K.T. Leung, S.N. Liss, B.-Q. Liao, Recent advances in membrane technologies for biorefining and bioenergy production, Biotechnol. Adv. 30 (2012) 817-858.
[16] B.K. Qi, J.Q. Luo, X.R. Chen, X.F. Hang, Y.H. Wan, Separation of furfural from monosaccharides by nanofiltration, Bioresource Technol. 102 (2011) 7111-7118.
[17] A. Teella, G.W. Huber, D.M. Ford, Separation of acetic acid from the aqueous fraction of fast pyrolysis bio-oils using nanofiltration and reverse osmosis membranes, J. Membrane Sci. 378 (2011) 495-502.
[18] Y.-H. Weng, H.-J. Wei, T.-Y. Tsai, W.-H. Chen, T.-Y. Wei, W.-S. Hwang, C.-P. Wang, C.-P. Huang, Separation of acetic acid from xylose by nanofiltration, Sep. Purif. Technol. 67 (2009) 95-102.
[19] F.L. Zhou, C.W. Wang, J. Wei, Separation of acetic acid from monosaccharides by NF and RO membranes: Performance comparison, J. Membrane Sci. 429 (2013) 243-251.
[20] T. Bras, V. Guerra, I. Torrado, P. Lourenco, F. Carvalheiro, L.C. Duarte, L.A. Neves, Detoxification of hemicellulosic hydrolysates from extracted olive pomace by diananofiltration, Process Biochem. 49 (2014) 173-180.
[21] J. Luo, B. Zeuner, S.T. Morthensen, A.S. Meyer, M. Pinelo, Separation of phenolic acids from monosaccharides by low-pressure nanofiltration integrated with laccase pre-treatments, J. Membrane Sci. 482 (2015) 83-91.
[22] S.K. Maiti, Y.L. Thuyavan, S. Singh, H.S. Oberoi, G.P. Agarwal, Modeling of the separation of inhibitory components from pretreated rice straw hydrolysate by nanofiltration membranes, Bioresource Technol. 114 (2012) 419-427.
[23] M. Malmali, J.J. Stickel, S.R. Wickramasinghe, Sugar concentration and detoxification of clarified biomass hydrolysate by nanofiltration, Sep. Purif. Technol. 132 (2014) 655-665.
[24] N. Nguyen, C. Fargues, W. Guiga, M.-L. Lameloise, Assessing nanofiltration and reverse osmosis for the detoxification of lignocellulosic hydrolysates, J.Membrane Sci. 487 (2015) 40-50.
[25] J.Q. Luo, L.H. Ding, X.G. Chen, Y.H. Wan, Desalination of soy sauce by nanofiltration, Sep. Purif. Technol. 66 (2009) 429-437.
[26] J.Q. Luo, Y.H. Wan, Desalination of effluents with highly concentrated salt by nanofiltration: From laboratory to pilot-plant, Desalination 315 (2013) 91-99.
[27] R. Paulen, M. Fikar, G. Foley, Z. Kovacs, P. Czermak, Optimal feeding strategy of diafiltration buffer in batch membrane processes, J. Membr. Sci. 411 (2012) 160-172.
[28] L.Y. Wang, G. Yang, W.H. Xing, N.P. Xu, Mathematic model of the yield for diafiltration processes, Sep. Purif. Technol. 59 (2008) 206-213.
[29] T.N.N. Nguyen Dinh, Detoxification of ligno-cellulosic hydrolyzates by pressure-driven membrane processes: interest of nanofiltration in a diafiltration mode, in Thèse en Génie des Procédés. 2014, AgroParisTech: Massy, France. p. 201.
[30] A.A. Alturki, N. Tadkaew, J.A. McDonald, S.J. Khan, W.E. Price, L.D. Nghiem, Combining MBR and NF/RO membrane filtration for the removal of trace organics in indirect potable water reuse applications, J. Membrane Sci. 365 (2010) 206-215.
[31] Y. Bennani, K. Kosutic, E. Drazevic, M. Rozic, Wastewater from wood and pulp industry treated by combination of coagulation, adsorption on modified clinoptilolite tuff and membrane processes, Environ. Technol. 33 (2012) 1159-1166.

[32] L.D. Nghiem, S. Hawkes, Effects of membrane fouling on the nanofiltration of pharmaceutically active compounds (PhACs): Mechanisms and role of membrane pore size, Sep. Purif. Technol. 57 (2007) 176-184.
[33] E. Sjoman, M. Manttari, M. Nystrom, H. Koivikko, H. Heikkila, Separation of xylose from glucose by nanofiltration from concentrated monosaccharide solutions, J. Membrane Sci. 292 (2007) 106-115.
[34] J. Warczok, M. Ferrando, F. Lopez, C. Guell, Concentration of apple and pear juices by nanofiltration at low pressures, J. Food Eng. 63 (2004) 63-70.
[35] E. Siversten, Membrane separation of anions in concentrated electrolytes, in Department of Chemical Engineering. 2001, Norwegian University of Science and Technology (NTNU), Norway: Trondheim. p. 232.
[36] L. Braeken, B. Bettens, K. Boussu, P. Van der Meeren, J. Cocquyt, J. Vermant, B. Van der Bruggen, Transport mechanisms of dissolved organic compounds in aqueous solution during nanofiltration, J. Membrane Sci. 279 (2006) 311-319.
[37] C.Y.Y. Tang, Y.N. Kwon, J.O. Leckie, Effect of membrane chemistry and coating layer on physiochemical properties of thin film composite polyamide RO and NF membranes I. FTIR and XPS characterization of polyamide and coating layer chemistry, Desalination 242 (2009) 149-167.
[38] M.M. Ferreira, M.C. LoureiroDias, V. Loureiro, Weak acid inhibition of fermentation by Zygosaccharomyces bailii and Saccharomyces cerevisiae, Int. J. Food Microbiol. 36 (1997) 145-153.
[39] E. Palmqvist, B. Hahn-Hägerdal, M. Galbe, G. Zacchi, The effect of water-soluble inhibitors from stream-pretreated willow on enzymatic hydrolysis and ethanol fermentation, Enzyme Microb. Technol. 19 (1996) 470-476.
[40] J. Wright, E. Bellissimi, E. de Hulster, A. Wagner, J.T. Pronk, A.J.A. van Maris, Batch and continuous culture-based selection strategies for acetic acid tolerance in xylose-fermenting Saccharomyces cerevisiae, Fems Yeast Res. 11 (2011) 299-306.
[41] H.K. Lonsdale, U. Merten, R.L. Riley, Transport properties of cellulose acetate osmotic membranes, J. Appl. Polym. Sci. 9 (1965) 1341-1362.
[42] A.A. Merdaw, A.O. Sharif, G.A.W. Derwish, Water permeability in polymeric membranes, Part I, Desalination 260 (2010) 180-192.
[43] E. Räsänen, M. Nyström, J. Sahlstein, O. Tossavainen, Comparison of commercial membranes in nanofiltration of sweet whey, Lait 82 (2002) 343-356.
[44] R. Salcedo-Diaz, P. Garcia-Algado, M. Garcia-Rodriguez, J. Fernandez-Sempere, F. Ruiz-Bevia, Visualization and modeling of the polarization layer in crossflow reverse osmosis in a slit-type channel, J. Membrane Sci. 456 (2014) 21-30.
[45] A. Farhat, F. Ahmad, N. Hilal, H.A. Arafat, Boron removal in new generation reverse osmosis (RO) membranes using two-pass RO without pH adjustment, Desalination 310 (2013) 50-59.
[46] R. Kumar, P. Bhakta, S. Chakraborty, P. Pal, Separating Cyanide from Coke Wastewater by Cross Flow Nanofiltration, Separ. Sci. Technol. 46 (2011) 2119-2127.
[47] Y.H. Weng, H.J. Wei, T.Y. Tsai, W.H. Chen, T.Y. Wei, W.S. Hwang, C.P. Wang, C.P. Huang, Separation of acetic acid from xylose by nanofiltration, Sep. Purif. Technol. 67 (2009) 95-102.
[48] Y.H. Weng, H.J. Wei, T.Y. Tsai, T.H. Lin, T.Y. Wei, G.L. Guo, C.P. Huang, Separation of furans and carboxylic acids from sugars in dilute acid rice straw hydrolyzates by nanofiltration, Bioresource Technol. 101 (2010) 4889-4894.
[49] D.V. Cortez, I.C. Roberto, Individual and interaction effects of vanillin and syringaldehyde on the xylitol formation by Candida guilliermondii, Bioresource Technol. 101 (2010) 1858-1865.

[50] T.T.M. Nguyen, A. Iwaki, Y. Ohya, S. Izawa, Vanillin causes the activation of Yap1 and mitochondrial fragmentation in Saccharomyces cerevisiae, J. Biosci. Bioeng. 117 (2014) 33-38.
[51] L. Deng, Y. Wang, Y. Zhang, R. Ma, The enhancement of ammonia pretreatment on the fermentation of rice straw hydrolysate to xylitol, J. Food Biochem. 31 (2007) 195-205.
[52] A.M. Shupe, S. Liu, Ethanol fermentation from hydrolysed hot-water wood extracts by pentose fermenting yeasts, Biomass Bioener.39 (2012) 31-38.
[53] T.-Y. Lee, M.-D. Kim, K.-Y. Kim, K. Park, Y.-W. Ryu, J.-H. Seo, A parametric study on ethanol production from xylose by *Pichia stipitis*, Biotechnol. Bioproc. E. 5 (2000) 27-31.

Figure captions

Figure 1. Scheme of the spiral-wound RO bench scale device (Polymem - France) – Batch recycling mode

Figure 2. Schematic representation of diafiltration settings

Figure 3. Pure water flux study (F_f = 400 L h^{-1}; T = 20°C).

Figure 4. Effect of pressure on solutes rejection: a) Inhibitors; b) Sugars.
Lines correspond to modeling for NF270 results according to Equation 10; (F_f = 400 L h^{-1}; T = 20°C; ΔP = 4, 6, 8, 10, 12, 14, 16 and 18 bar for NF270; ΔP = 5, 10, 15, 20, 25 bar for DK).

Figure 5. Effect of feed flow-rate on solutes rejection: a) Inhibitors ; b) Sugars.
(T= 20 °C; ΔP= 10 bar for NF270; ΔP = 15 bar for DK)

Figure 6. Effect of *VRR* increase on solutes rejection: a) Inhibitors; b) Sugars.
(F_f = 600 L h^{-1}; T = 20°C; ΔP = 10 bar and *VRR* = 1, 2, 4 for NF270; ΔP = 15 bar and *VRR* = 1, 2, 4, 8 for DK).

Figure 7. Glucose sorption isotherm for DK membrane (● sorption; ○ Desorption) and NF270 membrane (▲sorption; Δ Desorption).

Figure 8. Yeast growth study by turbidimetric assays (Bioscreen) on retentates obtained by nanofiltration in a concentration mode (DK membrane)

Figure 9. Feed concentration modification during diafiltration with NF270 and DK membranes: a) Inhibitors; b) Sugars.
Lines represent modeling for NF270 according to equation (12).
(F_f = 600 L h^{-1}; T = 20°C; ΔP = 10 bar for NF270; ΔP = 15 bar for DK)

Figure 10. Yeast growth study with flask assays on retentates obtained by nanofiltration in a diafiltration mode before (AD) and after (ADC8) concentration (DK membrane)